Monocyte-mediated regulation of genes by the amyloid and prion peptides in SH-SY5Y neuroblastoma cells

Beatriz Morte, Tamara Martínez, Alberto Zambrano and Angel Pascual

Instituto de Investigaciones Biomédicas. Consejo Superior de Investigaciones Científicas. Madrid. Spain.

Running Title:
Upregulation of genes by amyloid and prion peptides

Address correspondence:
Dr. A. Pascual
Instituto de Investigaciones Biomédicas. (C.S.I.C.).
Arturo Duperier, 4
28029 Madrid. Spain.
Tel. 34-91-585 4460 Fax. 34-91-585 4401
e-Mail: apascual@iib.uam.es

ABSTRACT

Alzheimer's disease as well as prion-related encephalopathies are neurodegenerative disorders of the central nervous system, which cause mental deterioration and progressive dementia. Both pathologies appear to be primarily associated with the pathological accumulation and deposit of β-amyloid or prion peptides in the brain, and it has been even suggested that neurotoxicity induced by these peptides would be associated to essentially similar pathogenic mechanisms, in particular to those that follow the activation of microglial cells. To probe whether the neurotoxic effects induced by the β-amyloid and prion peptides are actually mediated by similar glial-associated mechanisms, we have examined the differential expression of genes in SH-SY5Y neuroblastoma cells incubated with conditioned media from β-amyloid or prion-stimulated THP-1 monocytic cells. According to microarray analysis, not many coincidences are observed and only four genes (Hint3, Psph, Daam1 and c-Jun) appear to be commonly upregulated by both peptides. Furthermore, c-Jun appears to be involved in the cell death mediated by both peptides.

INTRODUCTION

Alzheimer and prion pathologies are neurodegenerative diseases characterized by the progressive loss of neuronal synaptic function, an effect that in both cases appears to be secondary to the toxicity induced by key proteins, the beta-amyloid (Aβ) in Alzheimer's disease and PrP in prion pathologies, which accumulate and aggregate in the brain. At first sight, both types of pathologies exhibit different specific characteristics in relation with the mode of transmission, the etiology, or the frequency of occurrence, and they can be considered as essentially distinct pathologies (Checler & Vincent, 2002).

However, despite these evident differences, these pathologies also show a number of similarities. In both cases neurodegeneration appears to be mediated by proteins that, as mentioned above, are aggregated and accumulated in the brain (Price *et al.*, 1993). Those proteins share a complex multi-domain structure and contain toxic sequences that mediate neurotoxicity and give rise to similar damaging apoptotic phenotypes (Checler & Vincent, 2002). Moreover, they share a number of properties such as the presence of metal-binding sites that mediate the binding of metals ions, in particular copper or zinc (Barnham *et al.*, 2006), or the existence of several repeats of a GxxxG motif in the transmembrane region, which contain a methionine residue that appears to be essential to modulate the neurotoxicity of Aβ in Alzheimer or the disease susceptibility in the prion associated pathologies (Barnham *et al.*, 2006). Evidence reported in those articles supported the hypothesis that neurotoxicity induced by both proteins, the amyloid and prion, would be mediated by similar, if not identical, molecular pathways and opened a very attractive possibility as is the use of common therapeutic strategies to treat and prevent Alzheimer's and prion diseases.

Unfortunately, this hypothesis appears to be too simplistic, and although it is evident that both the β-amyloid and the PrP proteins are neurotoxic and induce similar processes of apoptosis and neurodegeneration, the factors and pathways that mediate these effects could be essentially different (Forloni *et al.*, 1996; Hope *et al.*, 1996; Brown *et al.*, 1997). In this sense, we have also reported that both the amyloid-beta 25-35 (Aβ25-35) and the PrP106-126 fragments induce a distinct gene expression profile in the human SH-SY5Y neuroblastoma cell line. First, the number of genes significantly altered by

these treatments was markedly different, 198 in the case of the prion (Martinez & Pascual, 2007b), and 67 in the case of the amyloid fragment (Martinez & Pascual, 2007a), and second, the relationship between the overexpressed and repressed genes was opposite in both cases (16/182 and 54/13, respectively).

Despite this, it has been also well established that in addition to those effects directly induced on neurons, neurotoxicity of both peptides can be largely mediated by microglia activation, and the consequent release of cytotoxic molecules such as proinflammatory cytokines or reactive oxygen intermediates. In fact, an increasing body of evidence indicates that neuronal death induced by the β-amyloid and the prion peptides in the brain is mainly associated to processes that are promoted by activation of the surrounding microglial cells (Dheen *et al.*, 2007). To analyze possible coincidences between the neurotoxic effects induced by both peptides through activation of microglia, we have now analyzed the gene expression profile in SH-SY5Y neuroblastoma cells exposed to conditioned media obtained from Aβ25-35 or PrP106-126 stimulated THP-1 human monocytic cells, which were used as a surrogate model of human microglia.

MATERIALS AND METHODS

Cell Culture and treatments

Human monocytic THP-1 cells and SH-SY5Y human neuroblastoma cells were cultured as previously described (Combs *et al.*, 1999; Villa *et al.*, 2002) in RPMI 1640 medium supplemented with 10% fetal bovine serum (Gibco.Life technologies Ltd. Paislay. Scotland. UK), and maintained at 37ºC in a 5% CO2 atmosphere.

Synthetic Aβ25-35 obtained from AnaSpec and synthetic PrP106-126 obtained from Neosystem, were prepared as follows: Briefly, Aβ25-35 was dissolved in deionized-distilled water at a concentration of 2,5 mM and stored at −80 °C. Previous to the experiments, the stock solution was diluted to the desired concentrations and then added to the culture medium. The prion peptide 106-126 was dissolved in PBS at a concentration of 2 mM and maintained for 48 hours at room temperature to allow polymerization, before being added to the cells.

For experiments, THP-1 monocytes were incubated for 48 hours with or without 10 μM Aβ25-35 or 10 μM PrP106-126, and the conditioned media collected and centrifuged to eliminate cell residues. The cell-free supernatants were then used to replace the culture media of SH-SY5Y cells previously plated in 6-well plates and grown for 24 hours in RPMI/10%FBS media. Six hours after addition of conditioned media a set of cells was harvested for posterior RNA extraction and determination of gene expression. The remaining cells were incubated in the presence or in the absence of conditioned media for 24 hours and then photographed and fixed for histological analysis or collected and saved for subsequent protein or RNA extraction.

Fluorescence microscopy

SH-SY5Y cells were incubated for different time periods with the supernatants of amyloid- or prion-treated THP-1 cells or RPMI fresh medium, and then fixed with 4% paraformaldehyde at pH=7,4 and room temperature for 1 hour, permeabilized with 0,1% Triton-X-100, and then subjected to TUNEL assay to evaluate the cellular death by using the in situ cell death detection kit Fluorescein (Roche). To further confirm the findings of TUNEL assay, cells

were washed with PBS, stained with DAPI, and analyzed by fluorescence microscopy, using a Zeiss Axiophot inverted fluorescence microscope (515-565 nm for TUNEL, and 450-480 nm for DAPI). Images of cells were then digitized using an Olympus DP70 color camera.

MTT cell viability assay

Cell viability was evaluated in 96-well culture plates using a colorimetric assay based on the reduction of tetrazolium dye (MTT) to a blue formazan product. After incubation for 4 h with MTT (0.5 mg/ml) at 37°C, isopropanol/HCl was added to each 96-well and the absorbance of solubilized MTT formazan products was measured spectrophotometrically at 570 nm.

RNA interference

Expression of c-Jun in the SH-SY5Y cells was inhibited by using the Santa Cruz Biotechnology c-Jun siRNA (h2) (catalog number sc-44201). Cells were grown to 60% confluence and the c-Jun siRNA or a control siRNA (catalog number sc-37007) were transfected (using the transfection reagent sc-29528) according to the manufacturer's instructions. At 24 h after transfection, the medium was replaced and the cells were further incubated for 48 h. Next, media were removed and the cells were exposed to the THP-1 conditioned supernatants for 24 h.

RNA preparation and Microarray Analysis

For RNA isolation cell lysates were homogenized and the RNA purified by using the QIAshredder and RNeasy Mini kits of Qiagen, according to the manufacturer's recommendations. The final amount of isolated RNA was determined in each sample by spectrophotometry and its quality assessed by electrophoresis on agarose gels.

Preparation of cDNA, cRNA, hybridization and scanning of microarrays were performed following manufacturer's protocols. cDNA, and biotinylated cRNAs were synthesized from 5μg RNA samples with the GeneChip expression 3' amplification reagents (one-cycle cDNA synthesis, and IVT labelling) kits of Affymetrix, and biotinylated probes were hybridized to an Affymetrix gene chip human genome U133A Plus 2.0 array, a microarray that contains more than 54,000 probe sets and allows an accurate analysis of the quantitative expression of over 47,000 transcripts, including 38,500 well characterized human genes. Analysis for differential expression was performed using the R platform for statistical analysis (R Foundation for Statistical Computing. Vienna) and several packages from the Bioconductor project (Gentleman *et al.*, 2004; Carey *et al.*, 2005). The raw data were imported into R and pre-processed using the *affy* package and the robust multichip average method (Irizarry *et al.*, 2003). Genes were selected based on fold change. For this task an absolute fold change of 1.6 was used.

RT-PCR amplification of mRNA

RT-PCR was used to validate the differential expression of several Aβ- or PrP-responsive genes detected in the microarray analysis. Total RNA was extracted from cell cultures as mentioned above and cDNA was prepared from 250 ng of RNA using the high-capacity cDNA reverse transcription kit (Applied Biosystems, Foster City, CA). For quantitative PCR, a cDNA aliquot corresponding to 5 ng of the starting RNA was used, with Taqman Assay-on-Demand primers and the Taqman universal PCR master mix, No Amp Erase UNG (Applied Biosystems) on a 7900HT fast real-time PCR system (Applied Biosystems). The PCR program consisted in a hot start of 95 C for 10 min,

followed by 40 cycles of 15 sec at 95 C and 1 min at 60 C. PCRs were performed in triplicates, using the 18S gene as internal standard and the 2-cycle threshold method for analysis (Livak & Schmittgen, 2001).

Statistical analysis.

When appropriate, the significance of differences was calculated with the Student's t test, and it was indicated in the corresponding figure by the following symbol: $*$ $p < 0,05$ and ** $p< 0.01$.

RESULTS

Effects of the THP-1 conditioned medium on neuronal morphology and viability.

It is widely accepted that both the β-amyloid and prion peptides induce microglial activation and the subsequent secretion of cytokines and neurotoxic reactive oxygen species (Forloni *et al.*, 1993; Klegeris *et al.*, 1997), which in turn may increase neuronal apoptosis (Dheen *et al.*, 2007).

To further analyze and compare how the β-amyloid- and prion-stimulated microglia may affect neurons, we have exposed SH-SY5Y neuroblastoma cells to conditioned media obtained from THP-1 cells, a monocytic cell line that exhibits responses to stimuli similar to those of microglia (Combs *et al.*, 1999). THP-1 cells were incubated with or without 1,2 5 or 10μM Aβ25-35 or PrP106-126 for a 48 h time period and the recovered conditioned media was added to SH-SY5Y neuroblastoma cells that were then incubated for an additional 24 hours time period. The morphology and viability of cells were estimated by optical microscopy, TUNEL and DAPI staining (figure 1), and by MTT assay and Western blot analysis of caspase-3 (figure 2).

As illustrated in figure 1, morphology and viability of cells were not affected by conditioned medium from THP-1 cells treated with scrambled sequences, with 5μM Aβ25-35 or PrP106-126 (panel A), or with lower doses of those peptides. However, the cell morphology as well as the viability appeared to be severely affected after 24 hours of exposition to conditioned media from 10μM Aβ25-35 or PrP106-126 treated THP-1 cells (panel B). As shown in this panel, a large amount of neuroblastoma cells become apoptotic after 24 hours incubation with conditioned media from 10 μM Aβ25-35 or PrP106-126 treated cells. The number of cells was clearly reduced by both treatments and the residual cells became more rounded in appearance. Figure 2 includes the results obtained in a representative MTT assay (panel A), which confirms the reduced viability of cells, and the levels of activated caspase-3 detected by Western blot (panel B), which corroborated that apoptosis was significantly increased in SH-SY5Y cells incubated with those supernatants obtained from amyloid- or prion-stimulated THP-1 cells. All together, these results evidence that cell death was drastically increased in SH-SY5Y cells exposed for 24 hours to conditioned media recovered from amyloid- or prion-stimulated THP-1 cells.

Gene expression profile in SH-SY5Y cells incubated in THP-1 cells-conditioned culture media.

To analyze how the amyloid- and prion-activated microglia may affect the gene expression profiling in neurons, SH-SY5Y cells were exposed to conditioned media for a 6 hours time period and then harvested and saved for posterior RNA extraction and microarray analysis. Gene expression was analyzed by using an Affymetrix U133A plus2 array and the data analyzed as described under Materials and Methods.

As expected, both the amyloid- and prion-conditioned media induced changes on the gene expression profile of treated SH-SY5Y cells. A significance analysis of microarrays highlighted a relatively high number of transcripts differentially expressed in cells exposed to conditioned media from the THP-1 monocytic cells stimulated by the amyloid or prion fragments. However, the intensity of the response was rather low and not many genes change their expression by more than 1.6-fold. Of interest, the gene expression profiles appear to be different in both cases. First, the number of genes that change their expression appears to be much higher in amyloid-treated cells than in those cells exposed to the prion-conditioned medium. Second, whereas the genes affected by the prion-induced media appear to be mainly upregulated, the genes differentially expressed in cells exposed to the amyloid-conditioned media were largely down-regulated. These results are illustrated in the Venn diagram shown in figure 3, which outlines the total number of sequences up- and down-regulated, as well as the number of coincidences, detected in cells exposed to both treatments. As illustrated in this figure, a total of 168 sequences, 19 upregulated and 149 down-regulated, in cells exposed to the amyloid peptide-conditioned media, and a total of 17 sequences, all of them upregulated, in the cells treated with the prion-conditioned media, were found to be differentially expressed (above 1,6 fold with respect to control). After subtracting non annotated sequences and repeated probes the number of amyloid- and prion-induced genes were reduced to 141 (129 down- and 12 upregulated) and 11 (all of them upregulated), respectively. Furthermore, four of these sequences appeared to be commonly upregulated by both treatments.

The lists of the differentially expressed transcripts has been included in tables 1 (amyloid) and 2 (prion), which, as mentioned before, only include transcripts showing a 1,6-fold variation above or below the level found in the control.

Validation of the microarray data

To confirm the results obtained in the microarray analysis, the expression of a subset of genes selected from those identified in the microarray was analyzed by real-time PCR performed with cDNAs prepared from the RNAs of SH-SY5Y cells treated, or untreated, with conditioned media recovered from prion- or amyloid-stimulated THP-1 cells.

Transcripts chosen for confirmation included a total of 9 genes selected among those commonly deregulated by both the prion- and amyloid-conditioned media and/or because of their involvement in development and plasticity of the nervous system. As expected, the results from real-time PCR analysis were comparable to those provided by microarray analysis and, although in some of the samples the intensity of the response was different to that expected, all the transcripts analyzed showed the predicted differential expression patterns. Figure 4 shows the results obtained for five of these genes, two of them (JUN and DAAM1) commonly regulated by both treatments, and other three genes (STMN4, CREB5, and ETNK1) selected because of their contribution to the Jun-dependent signaling pathways. In agreement with the microarray data, four of these genes appear to be upregulated by both treatments, whereas ETNK1 that is down regulated in the amyloid treated cells remains unchanged in cells treated with the prion-stimulated medium. In addition, the differences obtained with the other analyzed genes (HINT3,

CREB1, BCLAF1 and MAP3K) were not significant, but also showed the same tendency observed in the microarrays (not shown).

c-Jun silencing decreases the monocytic-mediated cell death

To further prove the role of c-Jun in the apoptotic signals induced by the amyloid and prion peptides, we also analyzed the levels of activated caspase-3 and the cell viability in SH-SY5Y cells transfected with a specific c-Jun small interference RNA (c-Jun siRNA), which reduced c-Jun levels by about 50-60% (Figure 5). As shown in the panel A of this figure, the levels of cleaved caspase-3 were, as expected, increased in control cells transfected with a non-specific siRNA and exposed to supernatants recovered from the prion- or amyloid-stimulated THP-1cells. However, a significant decrease in caspase-3 cleavage was observed in SH-SY5Y cells transfected with the specific c-Jun siRNA, thus suggesting a role for this protein in the apoptotic pathways induced by both peptides. In addition, cell viability (MTT assay) was not significantly affected by c-Jun depletion in the absence of the peptide fragments, but the reduction of cell viability induced by the Aβ- or PrP-stimulated conditioned media was stronger in the c-Jun expressing cells than in the in the siRNA-transfected cells (panel B), further supporting a role for c-Jun in those processes.

DISCUSSION

Neurodegenerative diseases, in particular Alzheimer´s disease and prion associated pathologies have been shown to share a number of characteristics and it has been even suggested that neurotoxicity induced by both, the amyloid and prion proteins, would be mediated by similar, if not identical, molecular

pathways and mechanisms. In this sense, several factors have been already pointed as common targets of Aβ and prions (Ferreiro *et al.*, 2006; Ferreiro *et al.*, 2007; Lopes *et al.*, 2007), and common therapies based on these descriptions have been suggested (Checler & Vincent, 2002; Barnham *et al.*, 2006). In contrast, a number of discordances have been also described. As shown in a number of in vitro studies, Aβ and PrP peptides appear to induce neuronal apoptosis through different mechanisms (Forloni *et al.*, 1996; Hope *et al.*, 1996) (Brown *et al.*, 1997). Also in this line, we have described different gene expression profiles in neuroblastoma cells directly exposed to Aβ25-35 and PrP106-126 synthetic fragments (Martinez & Pascual, 2007b; a). However, in these reports we just described the effects directly induced by the prion and amyloid proteins on neurons, whereas neurotoxicity of both peptides has been proved to be further enhanced by the presence of glial (mostly microglial) cells (Dheen *et al.*, 2007). In fact, the number of glial cells has been described to correlate with the amyloid or prion deposition (Van Everbroeck *et al.*, 2004), and it has been suggested that activation of microglia by Aβ or PrP and the subsequent release of cytokines, reactive oxygen species and other neurotoxic factors would be the main cause of the enhanced apoptosis and neuronal death observed both in Alzheimer and prion diseases. To analyze possible coincidences in the microglia-mediated neuronal response to those peptides we have exposed neuroblastoma SH-SY5Y cells to conditioned media obtained from Aβ- or PrP-stimulated THP-1 monocytic cells, a established cell line widely used as a model for human microglia because of their functional similarities with primary microglia and their ability to activate similar signalling pathways (McDonald *et al.*, 1997; Combs *et al.*, 1999). As expected, exposure of

neuroblastoma cells to conditioned media from Aβ or PrP-treated THP-1 cells caused a significant increase of cell death that was clearly detectable by optical microscopy, and further proved by TUNEL staining and caspase-3 activation. In addition, we have also identified a number of genes whose expression appears to be deregulated in cells exposed to conditioned media. In both cases, it is noteworthy that amyloid-associated effects were always more evident that those induced by the prion-stimulated medium. First, the Aβ25-35 conditioned media appeared to be more toxic than that conditioned by PrP106-126 and apparently caused a higher lethality, as observed by optical microscopy. Second, in contrast to that observed when these peptides act directly on neurons (Martinez & Pascual, 2007b; a), the number of genes deregulated by Aβ25-35 was markedly higher than the number of genes affected by the prion-conditioned media. Indeed, whereas Aβ25-35-induced medium changes the expression of 141 genes by more than 1,6-fold with respect to the control group, only 11 genes were altered by the PrP106-126 fragment.

On the other hand, a comparative analysis of these results with those previously described in neuroblastoma cells directly exposed to the amyloid or prion fragments, shows a number of additional differences between the direct and macrophage-mediated effects induced by both peptides. So, whereas the amyloid fragment appears to activate similar pathways and processes both acting directly on neurons or indirectly through monocytic activation, the effects of the PrP106-126 peptide are largely different when exerted directly or indirectly on neurons.

Despite these marked differences, it is remarkable the common activation of four genes in cells exposed to both treatments; Hint3, which has not been

previously associated to neurodegenerative pathologies; Psph that is widely expressed in neuronal ganglia and Daam1 and c-Jun, which as previously described play a role in the developing and injured nervous system (Kida *et al.*, 2004; Zhou *et al.*, 2004). In particular, it results of interest the macrophage-mediated upregulation of c-JUN, a gene that has been associated to axon regeneration (Raivich *et al.*, 2004; Zhou *et al.*, 2004), to brain inflammation and to a wide number of processes involved in neuronal cell death and degeneration (Raivich, 2008). Moreover, a direct relationship between the JNK/c-Jun cascade and the Alzheimer's disease (Sun *et al.*, 2009) or prion-related pathologies (Lee *et al.*, 2005) has been suggested. In the present study the role of c-Jun in the apoptotic processes induced by the Aβ25-35 and PrP106-126 peptides has been confirmed by the reduced levels of cleaved caspase-3, an apoptotic marker, and the partial reversal of the cell viability reduction found in SH-SY5Y cells depleted of c-Jun by means of a specific siRNA.

In conclusion, our data show a number of divergences between the genes and mechanisms that mediate the neurotoxicity of Aβ and PrP peptides but, remarkably, also show the common activation of a reduced number of genes including c-Jun, which codes for a transcription factor largely involved in apoptotic processes. In this sense, PCR analysis also shows the upregulation of Creb5 a member of the CRE (cAMP response element)-binding protein family, which as previously reported (Dong *et al.*, 2007) may specifically interact with c-Jun and function as a CRE-dependent transactivator. These results further confirm previous descriptions about the role of c-Jun in neurodegenerative processes and reinforce the JNK/c-Jun pathway as a valuable target for the

development of common therapeutic strategies. However, it is also true that our experiments have been carried out using two established cell lines as models, and it could occur that they do not accurately reflect the microglial-mediated neuronal toxicity that both the amyloid and prion peptides exert in vivo. In any case, these results might contribute to increase the knowledge about the mechanisms that mediate the neurotoxicity of both the amyloid and the prion peptides and should be useful to develop new and specific multitargeted therapies for these diseases.

REFERENCES

Barnham, K.J., Cappai, R., Beyreuther, K., Masters, C.L. & Hill, A.F. (2006) Delineating common molecular mechanisms in Alzheimer's and prion diseases. *Trends Biochem Sci*, **31**, 465-472.

Brown, D.R., Herms, J.W., Schmidt, B. & Kretzschmar, H.A. (1997) PrP and beta-amyloid fragments activate different neurotoxic mechanisms in cultured mouse cells. *Eur J Neurosci*, **9**, 1162-1169.

Carey, V.J., Gentry, J., Whalen, E. & Gentleman, R. (2005) Network structures and algorithms in Bioconductor. *Bioinformatics*, **21**, 135-136.

Combs, C.K., Johnson, D.E., Cannady, S.B., Lehman, T.M. & Landreth, G.E. (1999) Identification of microglial signal transduction pathways mediating a neurotoxic response to amyloidogenic fragments of beta-amyloid and prion proteins. *J Neurosci*, **19**, 928-939.

Checler, F. & Vincent, B. (2002) Alzheimer's and prion diseases: distinct pathologies, common proteolytic denominators. *Trends Neurosci*, **25**, 616-620.

Dheen, S.T., Kaur, C. & Ling, E.A. (2007) Microglial activation and its implications in the brain diseases. *Curr Med Chem*, **14**, 1189-1197.

Dong, B., Kim, S., Hong, S., Das Gupta, J., Malathi, K., Klein, E.A., Ganem, D., Derisi, J.L., Chow, S.A. & Silverman, R.H. (2007) An infectious retrovirus susceptible to an IFN antiviral pathway from human prostate tumors. *Proc Natl Acad Sci U S A*, **104**, 1655-1660.

Ferreiro, E., Eufrasio, A., Pereira, C., Oliveira, C.R. & Rego, A.C. (2007) Bcl-2 overexpression protects against amyloid-beta and prion toxicity in GT1-7 neural cells. *J Alzheimers Dis*, **12**, 223-228.

Ferreiro, E., Resende, R., Costa, R., Oliveira, C.R. & Pereira, C.M. (2006) An endoplasmic-reticulum-specific apoptotic pathway is involved in prion and amyloid-beta peptides neurotoxicity. *Neurobiol Dis*, **23**, 669-678.

Forloni, G., Angeretti, N., Chiesa, R., Monzani, E., Salmona, M., Bugiani, O. & Tagliavini, F. (1993) Neurotoxicity of a prion protein fragment. *Nature*, **362**, 543-546.

Forloni, G., Bugiani, O., Tagliavini, F. & Salmona, M. (1996) Apoptosis-mediated neurotoxicity induced by beta-amyloid and PrP fragments. *Mol Chem Neuropathol*, **28**, 163-171.

Gentleman, R.C., Carey, V.J., Bates, D.M., Bolstad, B., Dettling, M., Dudoit, S., Ellis, B., Gautier, L., Ge, Y., Gentry, J., Hornik, K., Hothorn, T., Huber, W., Iacus, S., Irizarry, R., Leisch, F., Li, C., Maechler, M., Rossini, A.J., Sawitzki, G., Smith, C., Smyth, G., Tierney, L., Yang, J.Y. & Zhang, J. (2004) Bioconductor: open software development for computational biology and bioinformatics. *Genome Biol*, **5**, R80.

Hope, J., Shearman, M.S., Baxter, H.C., Chong, A., Kelly, S.M. & Price, N.C. (1996) Cytotoxicity of prion protein peptide (PrP106-126) differs in mechanism from the cytotoxic activity of the Alzheimer's disease amyloid peptide, A beta 25-35. *Neurodegeneration*, **5**, 1-11.

Irizarry, R.A., Hobbs, B., Collin, F., Beazer-Barclay, Y.D., Antonellis, K.J., Scherf, U. & Speed, T.P. (2003) Exploration, normalization, and summaries of high density oligonucleotide array probe level data. *Biostatistics*, **4**, 249-264.

Kida, Y., Shiraishi, T. & Ogura, T. (2004) Identification of chick and mouse Daam1 and Daam2 genes and their expression patterns in the central nervous system. *Brain Res Dev Brain Res*, **153**, 143-150.

Klegeris, A., Walker, D.G. & McGeer, P.L. (1997) Interaction of Alzheimer beta-amyloid peptide with the human monocytic cell line THP-1 results in a protein kinase C-dependent secretion of tumor necrosis factor-alpha. *Brain Res*, **747**, 114-121.

Lee, H.P., Jun, Y.C., Choi, J.K., Kim, J.I., Carp, R.I. & Kim, Y.S. (2005) Activation of mitogen-activated protein kinases in hamster brains infected with 263K scrapie agent. *J Neurochem*, **95**, 584-593.

Livak, K.J. & Schmittgen, T.D. (2001) Analysis of relative gene expression data using real-time quantitative PCR and the 2(-Delta Delta C(T)) Method. *Methods*, **25**, 402-408.

Lopes, J.P., Oliveira, C.R. & Agostinho, P. (2007) Role of cyclin-dependent kinase 5 in the neurodegenerative process triggered by amyloid-Beta and prion peptides: implications for Alzheimer's disease and prion-related encephalopathies. *Cell Mol Neurobiol*, **27**, 943-957.

Martinez, T. & Pascual, A. (2007a) Gene expression profile in beta-amyloid-treated SH-SY5Y neuroblastoma cells. *Brain Res Bull*, **72**, 225-231.

Martinez, T. & Pascual, A. (2007b) Identification of genes differentially expressed in SH-SY5Y neuroblastoma cells exposed to the prion peptide 106-126. *Eur J Neurosci*, **26**, 51-59.

McDonald, D.R., Brunden, K.R. & Landreth, G.E. (1997) Amyloid fibrils activate tyrosine kinase-dependent signaling and superoxide production in microglia. *J Neurosci*, **17**, 2284-2294.

Price, D.L., Borchelt, D.R. & Sisodia, S.S. (1993) Alzheimer disease and the prion disorders amyloid beta-protein and prion protein amyloidoses. *Proc Natl Acad Sci U S A*, **90**, 6381-6384.

Raivich, G. (2008) c-Jun expression, activation and function in neural cell death, inflammation and repair. *J Neurochem*, **107**, 898-906.

Raivich, G., Bohatschek, M., Da Costa, C., Iwata, O., Galiano, M., Hristova, M., Nateri, A.S., Makwana, M., Riera-Sans, L., Wolfer, D.P., Lipp, H.P., Aguzzi, A., Wagner, E.F. & Behrens, A. (2004) The AP-1 transcription factor c-Jun is required for efficient axonal regeneration. *Neuron*, **43**, 57-67.

Sun, K.H., Lee, H.G., Smith, M.A. & Shah, K. (2009) Direct and indirect roles of cyclin-dependent kinase 5 as an upstream regulator in the c-Jun NH2-terminal kinase cascade: relevance to neurotoxic insults in Alzheimer's disease. *Mol Biol Cell*, **20**, 4611-4619.

Van Everbroeck, B., Dobbeleir, I., De Waele, M., De Leenheir, E., Lubke, U., Martin, J.J. & Cras, P. (2004) Extracellular protein deposition correlates with glial activation and oxidative stress in Creutzfeldt-Jakob and Alzheimer's disease. *Acta Neuropathol*, **108**, 194-200.

Villa, A., Santiago, J., Garcia-Silva, S., Ruiz-Leon, Y. & Pascual, A. (2002) Serum is required for release of Alzheimer's amyloid precursor protein in neuroblastoma cells. *Neurochem Int*, **41**, 261-269.

Zhou, F.Q., Walzer, M.A. & Snider, W.D. (2004) Turning on the machine: genetic control of axon regeneration by c-Jun. *Neuron*, **43**, 1-2.

LEGEND TO THE FIGURES

Figure 1. Neurotoxic effects of the conditioned medium from cells treated with the 25–35 β-amyloid and 106–126 PrP fragments. SH-SY5Y cells were cultured for 24 h in the absence (control) or in the presence of conditioned media from β-amyloid- or prion-treated THP-1 monocytic cells, and the cell death was assessed by optical microscopy, DAPI staining and TUNEL analysis. Panel A illustrates results obtained with conditioned media from THP-1 cells treated with 5μM Aβ25–35 or PrP106–126 (left), or with 10μM of the corresponding scrambled peptides (right). Panel B shows the effects of conditioned media from THP-1 cells exposed to 10μM Aβ25–35 or PrP106–126.

Figure 2. Viability of SH-SY5Y cells incubated with or without THP-1 conditioned media. Cell death was evaluated by MTT assay or Western blot detection of activated caspase-3. Panel A illustrates the results obtained in a representative MTT assay performed in quadruplicate. Data (mean ± S.D) are expressed relative to the values obtained in control cells $^{**}P < 0.01$. Panel B shows the Western blot determination of cleaved caspase-3 and α-tubulin (loading control).

Figure 3. Venn diagram showing transcripts distribution between the amyloid and prion treated cells. The diagram was generated from lists of transcripts that are ≥1.6-fold up- (↑) or down- (↓) regulated by both treatments.

Figure 4. Validation of microarray data by quantitative reverse transcriptase polymerase chain reaction (RT-PCR). The differential expression of some genes identified in the microarray assay was analyzed by quantitative RT-PCR

carried out with RNA obtained from cells treated for 6 h with or without Aβ25-35- or PrP106–126-conditioned media. Data are expressed as fold change relative to control values obtained in untreated cells. *P < 0.05, **P < 0.01.

Figure 5. Silencing of c-Jun protects cells against Aβ and PrP toxicity. SH-SY5Y cells, transfected with a control (left) or a c-Jun specific siRNA (right), were incubated for 24 hours with conditioned media from β-amyloid or prion-stimulated THP-1 cells. Panel A illustrates the Western blot determination of c-Jun, cleaved caspase-3 and α-tubulin (loading control). Panel B illustrates the results obtained in a MTT assay performed in quadruplicate. Data (mean ± S.D) are expressed relative to the values obtained in cells transfected with the control siRNA in the absence of peptide fragments. ***P* < 0.01

Table 1. Deregulated genes in SH-SY5Y cells incubated for 6 hours with media conditioned by Aβ25-35-treated THP-1 cells. Table includes up and downregulated genes that change their expression by more than 1.6-fold with respect to the control group (Nonannotated or repeated genes have been excluded of this table).

Table 2. Deregulated genes in SH-SY5Y cells incubated for 6 hours with media conditioned by PrP106-126-treated THP-1 cells. Table includes upregulated genes that change their expression by more than 1.6-fold with respect to the control group. Not genes were found decreasing their expression by more than 1,6-fold. List does not included non annotated or repeated genes.

Figure 1

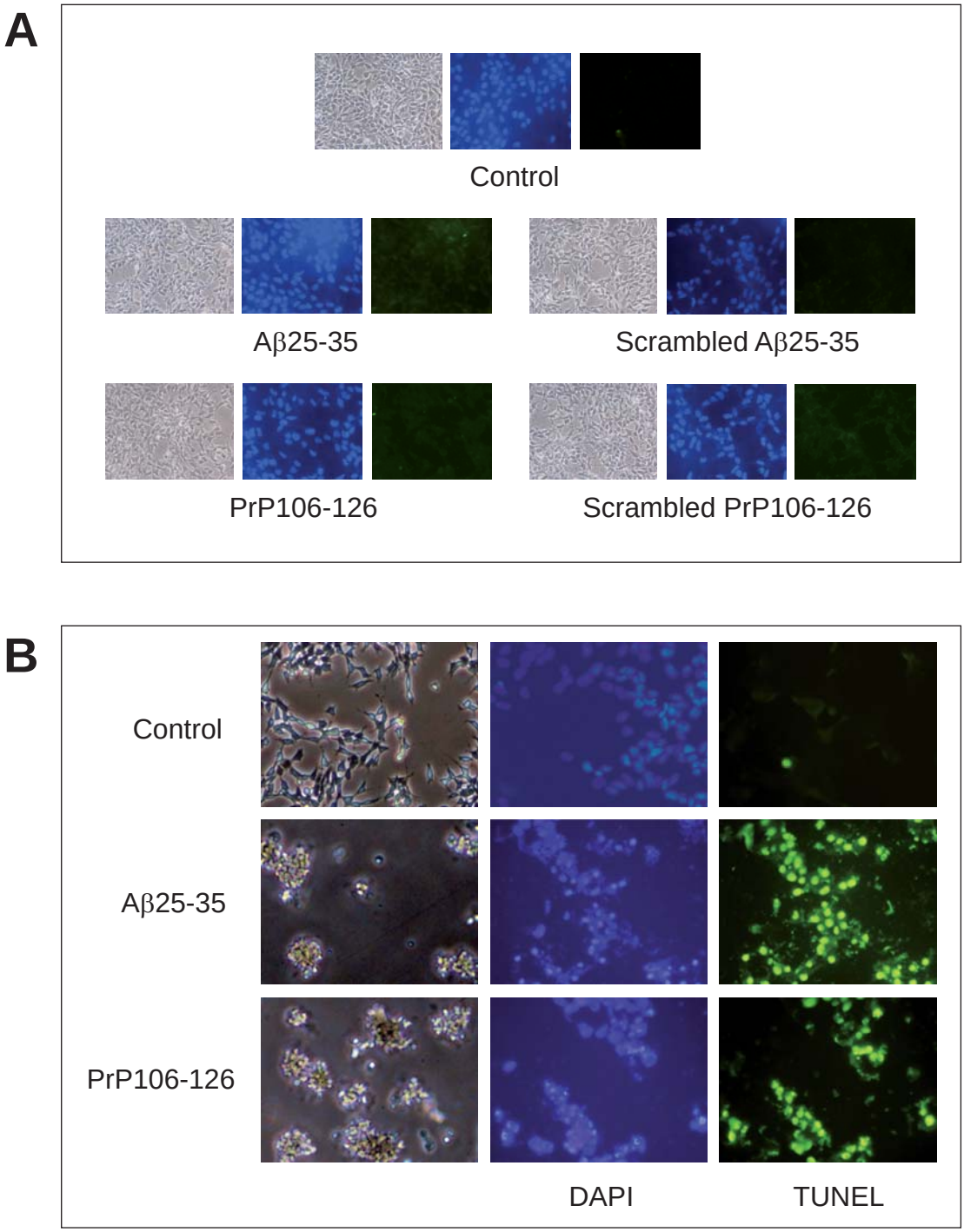
A
Control
Aβ25-35
Scrambled Aβ25-35
PrP106-126
Scrambled PrP106-126
B
Control
Aβ25-35
PrP106-126
DAPI
TUNEL

Figure 2

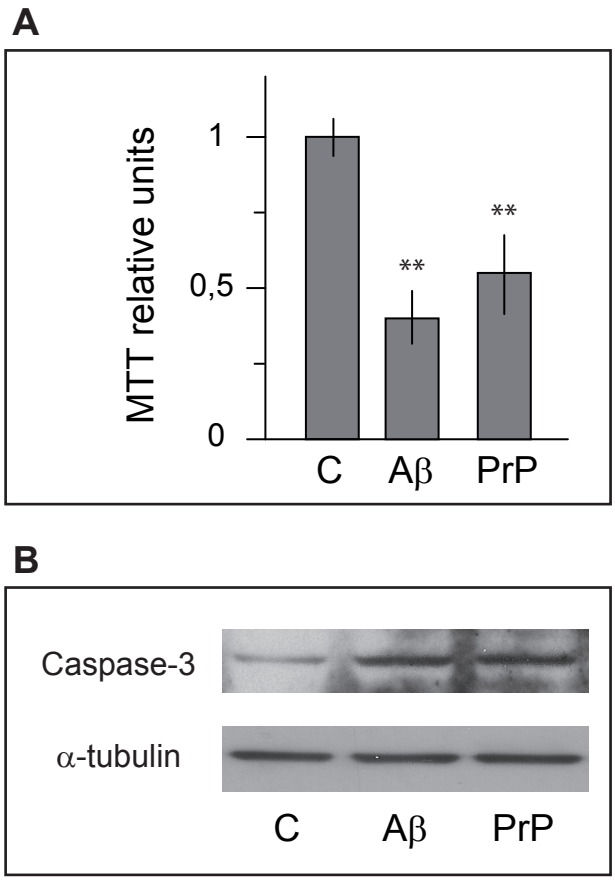
A
MTT relative units
1
0,5
0
**
**
C
Aβ
PrP
B
Caspase-3
α-tubulin
C
Aβ
PrP

Figure 3

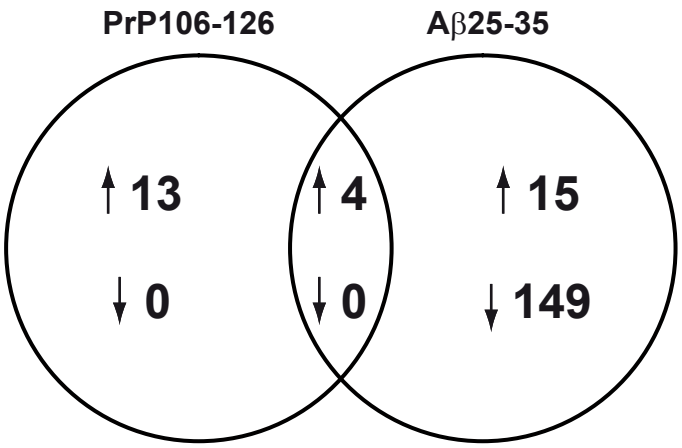

Figure 4

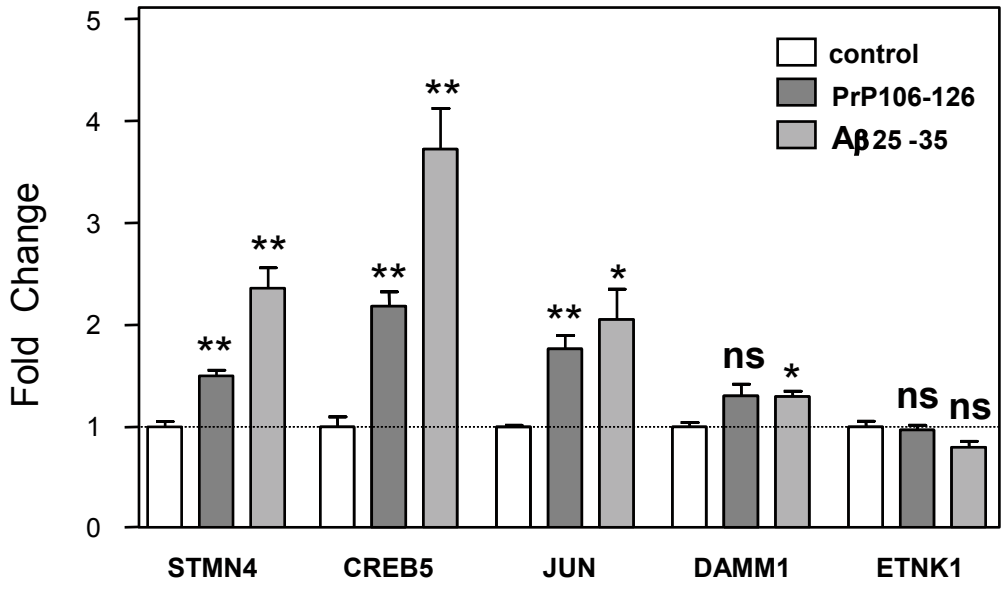
Fold Change
5
4
3
2
1
0
control
PrP106-126
Aβ25 -35
**
**
**
**
**
*
ns
*
ns
ns
STMN4
CREB5
JUN
DAMM1
ETNK1

Figure 5

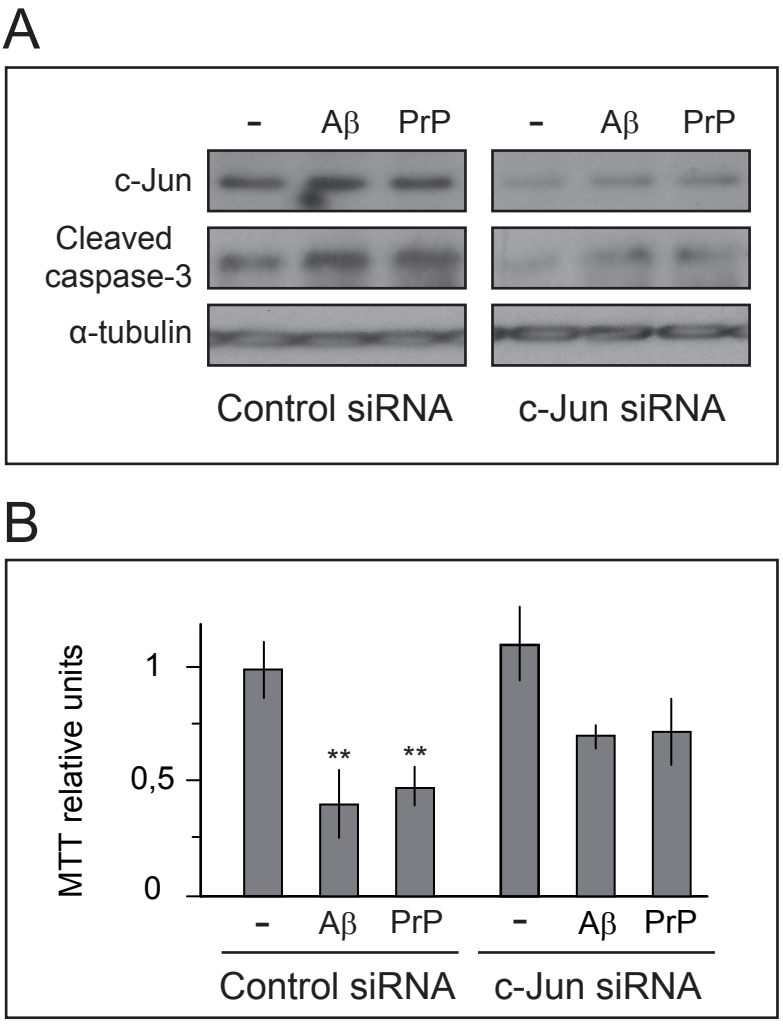
A
-
Aβ
PrP
-
Aβ
PrP
c-Jun
Cleaved caspase-3
α-tubulin
Control siRNA
c-Jun siRNA
B
MTT relative units
1
0,5
0
**
**
-
Aβ
PrP
-
Aβ
PrP
Control siRNA
c-Jun siRNA

Table 1. Deregulated genes in Aβ25-35-treated cells

Downregulated genes

Gene symbol	Gene name	Fold change
BCLAF1	BCL2-associated transcription factor 1	-2.35
TWF1	twinfilin, actin-binding protein, homolog 1 (Drosophila)	-2.31
GNA13	guanine nucleotide binding protein (G protein), alpha 13	-2.3
SCD	stearoyl-CoA desaturase (delta-9-desaturase)	-2.27
MALAT1	metastasis associated lung adenocarcinoma transcript 1	-2.2
SKP2	S-phase kinase-associated protein 2 (p45)	-2.19
ANKRD10	ankyrin repeat domain 10	-2.17
CDK6	cyclin-dependent kinase 6	-2.17
CEP170L	centrosomal protein 170kDa-like	-2.13
TAF9B	TAF9B RNA polymerase II, TATA box binding protein (TBP)-associated	-2.13
XIST	X (inactive)-specific transcript (non-protein coding)	-2.1
DCUN1D1	DCN1, defective in cullin neddylation 1, domain containing 1	-2.08
PTPN12	protein tyrosine phosphatase, non-receptor type 12	-2.08
COPA	coatomer protein complex, subunit alpha	-2.07
SUPT16H	suppressor of Ty 16 homolog (S. cerevisiae)	-2.07
PIK3C2A	phosphoinositide-3-kinase, class 2, alpha polypeptide	-2.06
PPAT	phosphoribosyl pyrophosphate amidotransferase	-2.06
SMC3	structural maintenance of chromosomes 3	-2.06
SCD	stearoyl-CoA desaturase (delta-9-desaturase)	-2.04
EXOC5	exocyst complex component 5	-2.02
SLC39A6	solute carrier family 39 (zinc transporter), member 6	-2
NUCKS1	nuclear casein kinase and cyclin-dependent kinase substrate 1	-1.99
GULP1	GULP, engulfment adaptor PTB domain containing 1	-1.97
PHTF2	putative homeodomain transcription factor 2	-1.97
CBX5	chromobox homolog 5 (HP1 alpha homolog, Drosophila)	-1.95
CLIC4	chloride intracellular channel 4	-1.95
CDC27	cell division cycle 27 homolog (S. cerevisiae)	-1.89
LOC100190986	hypothetical LOC100190986	-1.89
MEX3C	mex-3 homolog C (C. elegans)	-1.89
TMX1	thioredoxin-related transmembrane protein 1	-1.89
YTHDF3	YTH domain family, member 3	-1.88
EIF4A2	eukaryotic translation initiation factor 4A, isoform 2	-1.87
TMEM30A	transmembrane protein 30A	-1.87
BRCC3	BRCA1/BRCA2-containing complex, subunit 3	-1.85
EXOC4	exocyst complex component 4	-1.85
GTF2I	general transcription factor II, i	-1.85
JAM3	junctional adhesion molecule 3	-1.85
PNRC2	proline-rich nuclear receptor coactivator 2	-1.85
SCAMP1	secretory carrier membrane protein 1	-1.85
ZNF24	zinc finger protein 24	-1.85
C5orf22	chromosome 5 open reading frame 22	-1.84
CREB1	cAMP responsive element binding protein 1	-1.84
LARP4	La ribonucleoprotein domain family, member 4	-1.84
USP10	ubiquitin specific peptidase 10	-1.84
DHX9	DEAH (Asp-Glu-Ala-His) box polypeptide 9	-1.83
MCL1	myeloid cell leukemia sequence 1 (BCL2-related)	-1.83
NUDT21	nudix (nucleoside diphosphate linked moiety X)-type motif 21	-1.83
CD46	CD46 molecule, complement regulatory protein	-1.82
ACTR2	ARP2 actin-related protein 2 homolog (yeast)	-1.8
SLC16A1	solute carrier family 16, member 1 (monocarboxylic acid transporter 1)	-1.8

SRPK1	SFRS protein kinase 1	-1.8
VPS35	vacuolar protein sorting 35 homolog (S. cerevisiae)	-1.8
BCAT1	branched chain aminotransferase 1, cytosolic	-1.8
C10orf18	chromosome 10 open reading frame 18	-1.79
FYTTD1	forty-two-three domain containing 1	-1.79
WAC	WW domain containing adaptor with coiled-coil	-1.79
CPD	carboxypeptidase D	-1.78
IGF2BP3	insulin-like growth factor 2 mRNA binding protein 3	-1.78
MTPAP	mitochondrial poly(A) polymerase	-1.78
G3BP2	GTPase activating protein (SH3 domain) binding protein 2	-1.77
TOB1	transducer of ERBB2, 1	-1.77
UBXN4	UBX domain protein 4	-1.77
DDX3X	DEAD (Asp-Glu-Ala-Asp) box polypeptide 3, X-linked	-1.75
FAM29A	family with sequence similarity 29, member A	-1.75
JAK1	Janus kinase 1 (a protein tyrosine kinase)	-1.75
NFYA	nuclear transcription factor Y, alpha	-1.75
ANP32E	acidic (leucine-rich) nuclear phosphoprotein 32 family, member E	-1.74
EML4	echinoderm microtubule associated protein like 4	-1.74
IPO8	importin 8	-1.74
MAP3K1	mitogen-activated protein kinase kinase kinase 1	-1.74
CDV3	CDV3 homolog (mouse)	-1.73
DEPDC1	DEP domain containing 1	-1.73
PTAR1	protein prenyltransferase alpha subunit repeat containing 1	-1.73
RPRD1A	regulation of nuclear pre-mRNA domain containing 1A	-1.73
ZDHHC17	zinc finger, DHHC-type containing 17	-1.73
CCDC88A	coiled-coil domain containing 88A	-1.73
ATP13A3	ATPase type 13A3	-1.72
CBFB	core-binding factor, beta subunit	-1.72
GABRB3	gamma-aminobutyric acid (GABA) A receptor, beta 3	-1.72
MATR3	matrin 3	-1.72
PBRM1	polybromo 1	-1.72
PIP5K1A	phosphatidylinositol-4-phosphate 5-kinase, type I, alpha	-1.72
PREPL	prolyl endopeptidase-like	-1.72
RC3H2	ring finger and CCCH-type zinc finger domains 2	-1.72
RDX	radixin	-1.72
TEX15	testis expressed 15	-1.72
CANX	calnexin	-1.69
CCDC88A	coiled-coil domain containing 88A	-1.69
FAF1	Fas (TNFRSF6) associated factor 1	-1.69
SCAMP1	secretory carrier membrane protein 1	-1.69
APOOL	apolipoprotein O-like	-1.68
ELOVL2	elongation of very long chain fatty acids (FEN1/Elo2, SUR4/Elo3)-like 2	-1.68
GDAP1	ganglioside-induced differentiation-associated protein 1	-1.68
GLS	glutaminase	-1.68
HECTD1	HECT domain containing 1	-1.68
RAB35	RAB35, member RAS oncogene family	-1.68
DUSP6	dual specificity phosphatase 6	-1.67
HIPK1	homeodomain interacting protein kinase 1	-1.67
KIF5B	kinesin family member 5B	-1.67
MTMR1	myotubularin related protein 1	-1.67
SRPR	signal recognition particle receptor (docking protein)	-1.67
TIA1	TIA1 cytotoxic granule-associated RNA binding protein	-1.67
TMPO	thymopoietin	-1.67
ZNF146	zinc finger protein 146	-1.67
CASC5	cancer susceptibility candidate 5	-1.66
CNTN1	contactin 1	-1.66

CRKL	v-crk sarcoma virus CT10 oncogene homolog (avian)-like	-1.66
FNDC3A	fibronectin type III domain containing 3A	-1.66
MAT2A	methionine adenosyltransferase II, alpha	-1.66
UTRN	utrophin	-1.66
CDC2L5	cell division cycle 2-like 5 (cholinesterase-related cell division controller)	-1.65
CTDSPL2	CTD (carboxy-terminal domain, RNA polymerase II, polypeptide A) small	-1.65
ETNK1	ethanolamine kinase 1	-1.65
HNRNPU	heterogeneous nuclear ribonucleoprotein U (scaffold attachment factor A	-1.65
MBTPS2	membrane-bound transcription factor peptidase, site 2	-1.65
NARG2	NMDA receptor regulated 2	-1.65
RBM14	RNA binding motif protein 14	-1.65
TMEM194A	transmembrane protein 194A	-1.65
Sep-11	septin 11	-1.64
CACNA2D1	calcium channel, voltage-dependent, alpha 2/delta subunit 1	-1.64
G2E3	G2/M-phase specific E3 ubiquitin ligase	-1.64
NAMPT	nicotinamide phosphoribosyltransferase	-1.64
SNX13	sorting nexin 13	-1.64
ADAM10	ADAM metallopeptidase domain 10	-1.6
BAG4	BCL2-associated athanogene 4	-1.6
HSPH1	heat shock 105kDa/110kDa protein 1	-1.6
KCTD20	potassium channel tetramerisation domain containing 20	-1.6
MBNL1	muscleblind-like (Drosophila)	-1.6
RORB	RAR-related orphan receptor B	-1.6
	Upregulated genes	
STMN4	stathmin-like 4	2.3
CREB5	cAMP responsive element binding protein 5	2.28
HINT3	histidine triad nucleotide binding protein 3	1.92
JUN	jun oncogene	1.87
IDH2	isocitrate dehydrogenase 2 (NADP+), mitochondrial	1.83
DAAM1	dishevelled associated activator of morphogenesis 1	1.78
PSPH	phosphoserine phosphatase	1.73
AMOTL2	angiomotin like 2	1.72
METT10D	methyltransferase 10 domain containing	1.67
RAP2C	RAP2C, member of RAS oncogene family	1.67
C4orf30	chromosome 4 open reading frame 30	1.66
DUSP10	dual specificity phosphatase 10	1.64

Table 2. Deregulated genes in PrP106–126-treated cells

Upregulated genes

Gene symbol	Gene name	Fold change
HINT3	histidine triad nucleotide binding protein 3	1.91
SMA4	glucuronidase, beta pseudogene	1.89
SLITRK6	SLIT and NTRK-like family, member 6	1.77
DAAM1	dishevelled associated activator of morphogenesis 1	1.73
JUN	jun oncogene	1.68
C21orf45	chromosome 21 open reading frame 45	1.66
PSPH	phosphoserine phosphatase	1.65
GRIA2	glutamate receptor, ionotropic, AMPA 2	1.64
C15orf40	chromosome 15 open reading frame 40	1.64
LYZ	lysozyme (renal amyloidosis)	1.64

***Research Highlights**

In this paper we have analyzed the monocyte-mediated gene expression profile induced by the amyloid an prion peptides in the human SH-SY5Y neuroblastoma cell line. Results show a relevant coincidence in activating the expression of four genes Hint3, Psph, Daam1 and c-Jun. Furthermore, c-Jun appears to be involved in the cell death mediated by both peptides.

***Detailed Response to Reviewers**

Answers to reviewer 2

As requested, we have now included those results not illustrated or mentioned as not shown in the former manuscript. They are shown in the new figures 1 and 5, and a short description has been added into the text and legends.

- As indicated in our previous version “the effect was not induced by scrambled sequences and was not observed with doses of Aβ25-35 or PrP106-126 lower 5μM (data not shown)”. These results have been now included in figure 1A, although because their extension in the new figure we have just included the results corresponding to the higher dose of those compound, that is 5μM. Of course, if you consider it is necessary, we could also include the results obtained with the other doses tested (1 and 2 μM), that of course were also unable to reduce cell viability.

- In addition, the results obtained in the MTT assay have been included in figure 5. Now it is possible to observe how the reduction of cell viability induced by both fragments is partially reversed in cells transfected with the c-Jun siRNA, thus suggesting a role for Jun in those processes.